

# Miscibility, Microstructure, and Dynamics of Blends Containing Block Copolymer. 2. Microstructure of Blends of Homopolystyrene with Styrene–Butadiene Block Copolymers

Hanqiao Feng\* and Zhiliu Feng

*Polymer Physics Laboratory, Changchun Institute of Applied Chemistry, Chinese Academy of Sciences, Changchun 130022, People's Republic of China*

Lianfang Shen

*Laboratory of Magnetic Resonance and Atomic and Molecular Physics, Wuhan Institute of Physics, Chinese Academy of Sciences, Wuhan 430071, People's Republic of China*

*Received August 31, 1993; Revised Manuscript Received August 30, 1994\**

**ABSTRACT:** The microstructures of styrene–butadiene triblock (SBS) and styrene–butadiene four-arm star block (SB-4A) copolymers and their blends with homopolystyrene (PS) of different molecular weights,  $M_{PS}$ , have been investigated by means of small-angle X-ray scattering (SAXS) and  $^{13}C$  CP/MAS NMR. Quantitative analysis with SAXS indicates that the interdomain distance  $D$  increases with  $M_{PS}$  for miscible blends and is independent of  $M_{PS}$  for partially miscible blends with PS of a much higher  $M_{PS}$ , implying that PS with a much higher  $M_{PS}$  segregates in between the PS block microdomains as a new homogeneous phase. Meanwhile, the interfacial thickness,  $t$ , shows no dependence on the  $M_{PS}$ . The results from proton spin diffusion measurements for blends of SB-4A with PS of a much lower  $M_{PS}$  indicate that the interdomain size was decreased by the addition of PS, suggesting that there were detectable PS molecules dissolved in the PBD microdomains of SB-4A. Results from both SAXS and NMR are in good agreement for the pure block copolymers but are different for their blends with PS. NMR can give more reasonable microscopic pictures than SAXS for the studied polymer blends.

## Introduction

In this series of studies, the miscibility, morphology, and dynamics of blends of a styrene–butadiene four-arm star block (SB-4A) and styrene–butadiene–styrene triblock (SBS) copolymers with homopolystyrene (PS) of different molecular weights,  $M_{PS}$ , have been studied by dynamic mechanical analysis (DMA), small-angle X-ray scattering (SAXS), and NMR techniques in order to explore the relationship between microstructure and macroscopic mechanical properties of these blends. In part 1<sup>1</sup> of this series, the miscibilities of the blends of PS/SB-4A and PS/SBS were studied by DMA and  $^{13}C$  CP/MAS NMR. Some interesting results were obtained, such as a strong dependence of miscibility on  $M_{PS}$  but little on the molecular architecture of the block copolymers; intermolecular “entanglement” interaction being suggested as the reason for well-improved mechanical properties of the blends with PS of proper  $M_{PS}$ ; solubilization of PS in polybutadiene (PBD) domains; and PS still being miscible with the block copolymers, even when  $M_{PS}/M_{bPS}$  was as high as 1.2 and 1.5 for SB-4A and SBS, respectively.

In this work, the microstructures of the blends PS/SB-4A and PS/SBS have been quantitatively studied by SAXS and proton spin diffusion techniques. It is found that both SAXS and proton spin diffusion can quantitatively characterize the domain structures of these blends, such as interdomain distance, interfacial size, etc. However, for the polymer blends studied, NMR can give more reasonable microstructure data than SAXS.

## Experimental Section

The polymers used in this study were all commercial products. PS with different  $M_w$ 's were obtained from Nanjing

University; triblock (SBS) and four-arm star block (SB-4A) copolymers were obtained from the Synthetic Rubber Factory of Baling Petro-Chemical Co. and were purified before use. Solution blending was used in this study, using toluene as the solvent and a solution concentration of 5% (w/v).

Film specimens of PS/SBS and PS/SB-4A (20:80 by weight) were cast from their solution at 40 °C and then dried under vacuum at 60 °C until a constant weight was attained. The characteristic data of the polymers are listed in Tables 1 and 2.

Proton spin-diffusion experiments were performed on a Bruker MSL-400 NMR spectrometer at 298.0 K. The TOSS method was used for suppressing the spinning side band. The carbon resonance frequency was 100.63 MHz, and the proton resonance frequency was 400.3 MHz. A 4.8- $\mu$ s 90° pulse for the  $^{13}C$  nucleus and a 5.1- $\mu$ s 90° pulse for  $^1H$  were used. The Hartmann–Hahn cross-polarization matching field was about 49 kHz. The contact time (CT) was 1.0 ms. The delay time was 2 s. SAXS experiments were carried out on a Philips PW1700 automated powder diffractometer equipped with a Kratky SAXS camera. Ni-filtered Cu K $\alpha$  radiation with a wavelength of  $\lambda = 1.54$  Å was used (voltage 40 kV; current 30 mA).

## Results and Discussion

**A. Results of SAXS Measurements.** A SAXS technique has been used to study ordered microdomain structures of block copolymers and their blends with homopolymer.<sup>2–7</sup> It is well-known that the scattering intensity at large scattering angles for an isotropic pseudo-two-phase system is asymptotically given by the following equation:<sup>8</sup>

$$I(s) = (2\pi)^{-3} I_e (q_1 - q_2)^2 A_{int} s^{-4} \exp(-4\pi^2 \sigma^2 s^2) \quad (1)$$

where  $I_e$  is the Thomson scattering from an electron,  $A_{int}$  is the total interfacial area of the system, and  $\sigma$  is the parameter characterizing interfacial thickness,  $t$ , as follows:<sup>2,3</sup>

$$t = (2\pi)^{1/2} \sigma \quad (2)$$

\* To whom correspondence should be addressed. Present address: Laboratory of Magnetic Resonance and Atomic and Molecular Physics, Wuhan Institute of Physics, Chinese Academy of Sciences, Wuhan 430071, People's Republic of China.

† Abstract published in *Advance ACS Abstracts*, October 15, 1994.

**Table 1. Molecular Characteristics of Homopolystyrenes**

sample	$M_n \times 10^{-4}$	$M_w/M_n$	$T_g$ (K)
PS03	0.34	1.05	339.3
PS1	0.97	1.03	367.0
PS2	2.16	1.04	369.2
PS12	12.5	1.06	371.8
PS100	97.1	1.08	374.5

**Table 2. Molecular Characteristics of Block Copolymers**

sample	$M_n \times 10^{-4}$ <sup>a</sup>	SB <sup>b</sup> (w/w)	PS $M_n \times 10^{-4}$
SBS	6.70	44/56	1.47
SB-4A <sup>c</sup>	15.43	45/55	1.73

<sup>a</sup> Determined by membrane osmometry in toluene at 37 °C.

<sup>b</sup> Determined by <sup>13</sup>C NMR. <sup>c</sup> PS blocks locate at the outer end of the copolymer chains.

The intensity is corrected for the background scattering  $I_b$ . For an ideal two-phase system, the intensity  $I(s)$  is proportional to  $s^{-4}$ .<sup>9</sup>

From eq 1 one can estimate the parameter  $\sigma$  related to the interfacial thickness from the slope of the plot of  $\ln[s^4 I(s)]$  vs  $s^2$ . Thus, the interfacial thickness  $t$  can be obtained from eq 2, and the interdomain distance  $D$  was determined by using Bragg's equation

$$2D \sin \theta_m = \lambda \quad (3)$$

where  $2\theta_m$  is the scattering angle where the scattering becomes maximum, and  $\lambda$  is the wavelength of the X-ray.

Shown in Figure 1a–f are the desmeared SAXS curves of SB-4A and its blends with PS of different  $M_w$ 's after correction for background and absorption. In the figure, there are several points deserving mention. First, the positions of the scattering maxima of different blends are different. As compared with pure SB-4A block copolymer, the scattering peak positions of the miscible blends with PS03, PS1, and PS2 shift toward smaller angles. At the same time, the higher the molecular weight of the PS, the smaller the scattering angle  $2\theta$  (Figure 1b–d). The situation is markedly different for the partially miscible blends of SB-4A with PS12 and with PS100. The scattering peak positions of these two blends are the same as that of pure SB-4A copolymer. According to eq 3, the shifting of the scattering peak position toward smaller angles indicates that the interdomain distance of SB-4A has been enlarged by the addition of PS, implying that the added PS is well mixed with the PS block phase of SB-4A. However, the addition of higher molecular weight PS, such as PS12 or PS100, into SB-4A has no effect on the scattering peak position of SB-4A, which suggests that there is no detectable amount of PS being mixed with the PS blocks of SB-4A within experimental error. Therefore, it may be considered that the added PS forms another "homogeneous" phase; i.e., phase separation occurs, that will not give rise to scattering of X-rays. Hence, no change of the scattering peak position of the SB-4A occurred. Second, SB-4A and its blends with PS show higher order scattering maxima at  $2\theta$  around 0.6–0.8, and their positions and relative peak heights strongly depend on the molecular weights of PS. Multiple peaks in SAXS are interpreted as higher-order reflection of the same entity, and the number of scattering maxima depends on the uniformity of the domain spacing.<sup>2,10</sup> The relative peak heights of higher order SAXS maxima are known to be a function of the volume fraction of one type of lamellar microdomain.<sup>11</sup> Therefore, the change of the relative peak height with the

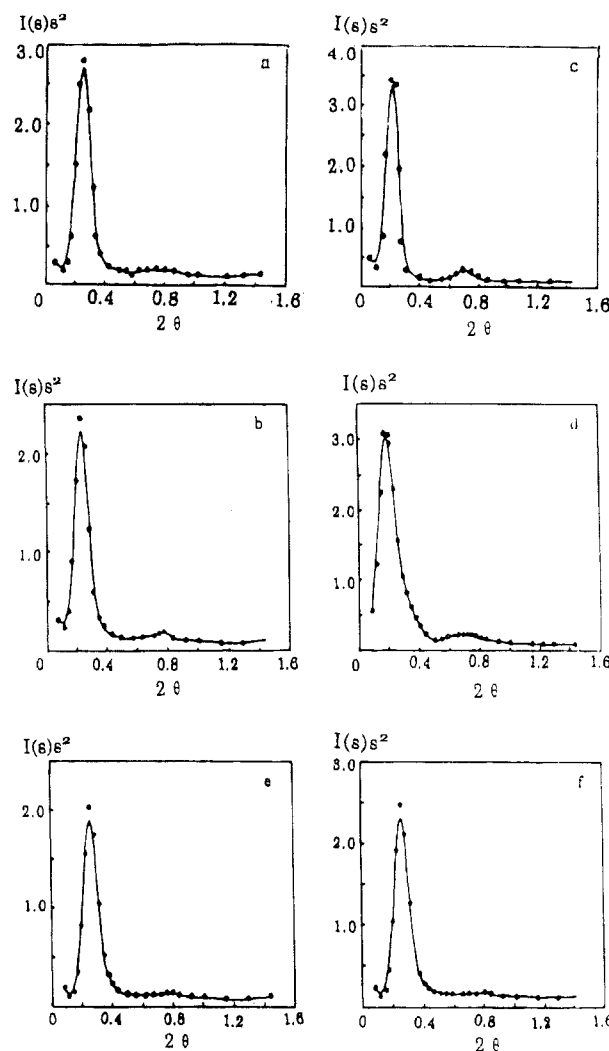


**Figure 1.** Desmeared SAXS curves of SB-4A and its blends with PS: (a) SB-4A; (b) PS03/SB-4A; (c) PS1/SB-4A; (d) PS2/SB-4A; (e) PS12/SB-4A; (f) PS100/SB-4A.

addition of PS indicates the change of the relative volume of the two types of lamellae (i.e., PS and PBD lamellae), which, in turn, implies the solubilization of PS into the microdomain space. The fact that the relative peak heights are different for different blends means that the amount of PS solubilized in the microdomain space varies with the molecular weight of PS. From the curves shown in Figure 1, it is seen that the relative peak heights of the blends are higher than that of pure SB-4A and the relative peak heights of the miscible blends are higher than those of the partially miscible blends. So the higher the molecular weight of PS, the lower the relative peak height of its blends with SB-4A. This means that the lower the molecular weight of PS, the more the amount of PS solubilized into the microdomain space of SB-4A, which is in good agreement with the results of the DMA experiment.<sup>1</sup>

It is interesting to find that the interdomain distances calculated by eq 3 are longer than those determined by the position of the peak maximum of the correlation function. The correlation function is defined as the probability that two volume units (or points)  $i$  and  $j$ , separated by a distance  $r$ , have the same electron density.<sup>11,12</sup> The correlation function will have maxima that reflect the positions of the repeat distances and contain information from all parts of the scattering systems. Besides, the correlation function often shows more readily discernible maxima than the original

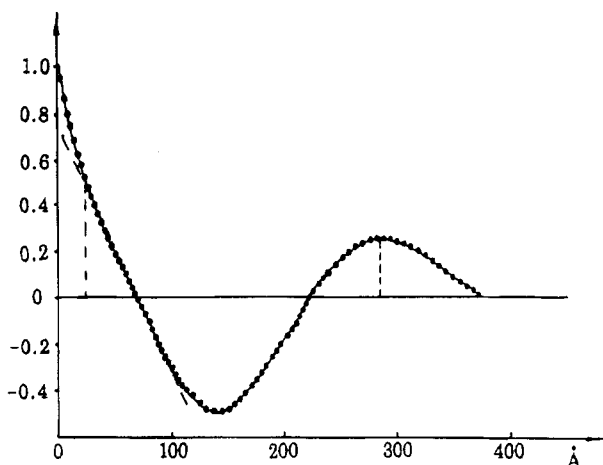


**Figure 2.** Correlation function of SB-4A calculated from the data from Figure 1.

**Table 3. Domain Properties of SB-4A and Its Blends<sup>a</sup> with PS from SAXS**

material	domain properties				
	$D^b$ (nm)	$D^c$ (nm)	$t^d$ (nm)	$t^e$ (nm)	$f$
SB-4A	34.2	28.8	$2.4 \pm 0.2$	$2.4 \pm 0.2$	0.14
PS03/SB-4A	38.5	30.6	$2.3 \pm 0.2$	$2.3 \pm 0.2$	0.12
PS1/SB-4A	44.0	33.6	$2.5 \pm 0.2$	$2.5 \pm 0.2$	0.11
PS2/SB-4A	51.1	38.1	$2.5 \pm 0.2$	$2.5 \pm 0.2$	0.09
PS12/SB-4A	34.2	27.9	$2.4 \pm 0.2$	$2.4 \pm 0.2$	0.14
PS100/SB-4A	34.2	28.0	$2.4 \pm 0.2$	$2.5 \pm 0.2$	0.13

<sup>a</sup> Composition of PS/SB-4A: 20/80. <sup>b</sup> Calculated by eq 3. <sup>c</sup> Calculated by the position of the peak maximum of the correlation function. <sup>d</sup> Calculated by eqs 2 and 4. <sup>e</sup> Determined from the lower limit of the straight section in the self-correlation range.

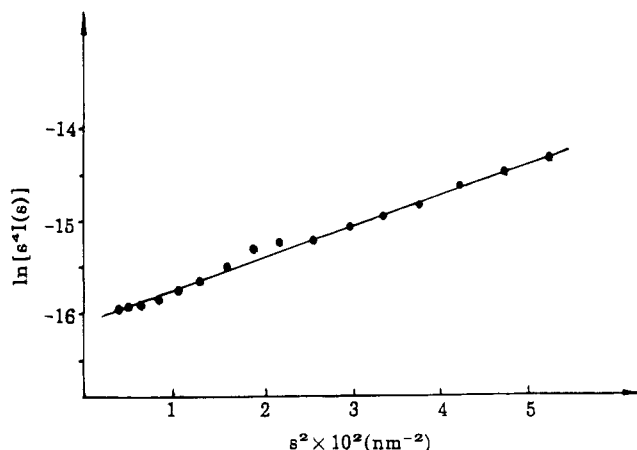


**Figure 3.** Typical plot of  $\ln[s^4 I(s)]$  vs  $s^2$  from the full analysis on the desmeared data of SB-4A.

scattering curves. Shown in Figure 2 is the correlation function calculated from the data from Figure 1. According to the correlation function of SB-4A and its blends with PS of different  $M_{PS}$ , it is found that addition of PS into SB-4A affects not only the microdomain size but also the spatial arrangement of the domains and the distribution of the domain size. Among them PS2 has the greatest effect on the microstructures of SB-4A. Besides, even for blends of PS12/SB-4A and PS100/SB-4A, their electron densities also changed to some degree by the addition of PS. The characteristics of microdomain structures for SB-4A and its blends with PS are listed in Table 3.

Figure 3 shows a typical plot of  $\ln[s^4 I(s)]$  vs  $s^2$  from the full analysis on the desmeared data of SB-4A. From the slope, the parameter  $\sigma$  related to the interfacial thickness can be estimated. Hence, the interfacial

**Table 4. Domain Properties of SB-4A and Its Blends<sup>a</sup> with PS**

material	SD time(s)	morphology	domain properties			
			$D^b$ (nm)	$t^b$ (nm)	$D^c$	$t^c$ (nm)
SB	0.0044	lamellae	23.9	$1.9 \pm 0.2$	28.8	$2.4 \pm 0.2$
	3.1749	cylinder	33.8	$2.7 \pm 0.2$		
PS03/SB-1A	0.0025	lamellae	11.5	$1.4 \pm 0.2$	30.6	$2.3 \pm 0.2$
	0.7349	cylinder	16.3	$2.0 \pm 0.2$		
PS100/SB-4A	0.0031	lamellae	27.6	$1.6 \pm 0.2$	28.0	$2.5 \pm 0.2$
	4.2208	cylinder	38.9	$2.2 \pm 0.2$		

<sup>a</sup> Composition of PS/SB-4A: 20/80. <sup>b</sup> Determined by spin proton diffusion. <sup>c</sup> Determined from SAXS.

thickness,  $t$ , can be obtained from eq 2. The  $t$  values of SB-4A and its blends with PS are also listed in Table 3.

However, we consider that there should exist some relationship in another form among these parameters as follows:

$$I(s)_{\text{obsd}} = (\text{const})s^{-4} \exp(4\pi^2 \sigma^2 s^2) \quad (4)$$

which can be used to estimate the parameter  $\sigma$  related to the interfacial thickness from the slope of the  $\ln[s^4 I(s)]$  vs  $s^2$  (see Figure 3). Here,  $I_{\text{obsd}}$  is the desmeared datum at large scattering angles. Equation 4 is at least a good approximation for the case we are discussing here. It is found that the  $t$  values obtained from eqs 2 and 4 are in good agreement with those from the lower limit of the straight section (see Figure 2 and Table 3) in the self-correlation range and with those from NMR measurements (see Table 4).

There are several points about the interfacial thickness deserving mention. (1) The interfacial thickness is almost independent of the molecular weight (from  $10^3$  to  $10^6$ ) of PS. (2) The volume fraction of the interfacial region  $f$  systematically decreases with increasing  $M_{PS}$  for the miscible blends but stays constant for the partially miscible blends.

**B. Proton Spin Diffusion in SB-4A and Its Blends with PS.** Proton spin diffusion has been used to detect the homogeneity of polymer systems.<sup>13-16</sup> Usually, the mean-square displacement of spin diffusion during time  $t$  is given by<sup>17</sup>

$$\langle X \rangle^2 = (4/3)Dt \quad (5)$$

and the maximum diffusive path length  $X$  can be calculated by the following equation:<sup>13</sup>

$$\langle X \rangle^2 = 2dDt \quad (6)$$

where  $d$  is the spatial dimension of the domain and takes the values of 1, 2, and 3 for lamellae, cylinders, and spheres, respectively, and  $D$  is the spin diffusion coefficient, which can be calculated by<sup>4</sup>

$$D = 2r_0^2/T_2 \quad (7)$$

where the hydrogen van der Waals radius of 1.17 Å is used for  $r_0$ <sup>14,18</sup> while  $T_2$  is the spin-spin relaxation time of the slowly decaying components. Having obtained the values of  $T_2$  and  $t$  of the studied systems, one can use the above equations to calculate the domain sizes in heterogeneous systems.

In this work, an extended Goldman-Shen pulse sequence<sup>15</sup> was used to detect the proton spin diffusion in SB-4A and its blends with PS. Some interesting results are obtained.

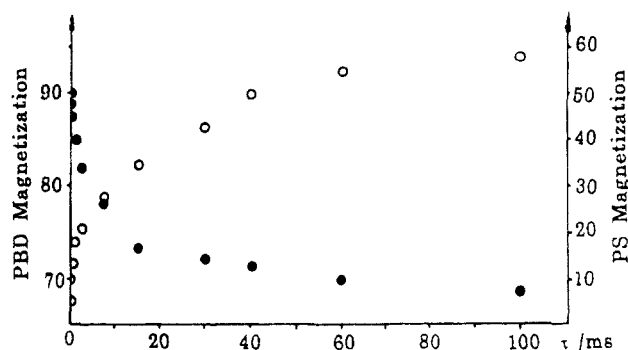


**Figure 4.** Magnetization changes of PS and PBD as a result of spin diffusion from PBD to PS: (○) for PS; (●) for PBD.

Figure 4 shows the changes of magnetizations of PS and PBD block in pure SB-4A with mixing time  $\tau$ . A transfer of magnetization from PBD to PS is obviously observed. The spin diffusion times  $t$  obtained from a biexponential fit of the curve are listed in Table 4. The short spin diffusion time can be explained as coming from the transfer of magnetization between PS and PBD at the interface, and the long time can be assigned to the spin diffusion between the PS domains and PBD domains. The  $T_2$  values of PBD in the interfacial region and pure PBD domains are 60 and 320  $\mu\text{s}$ , respectively, and the corresponding  $D$  values are  $4.0 \times 10^{-12}$  and  $0.9 \times 10^{-12} \text{ cm}^2/\text{s}$ , calculated according to eq 7. The domain sizes of SB-4A and its blends with PS, which were calculated with eq 6, are listed in Table 4. The sizes of the domains, obtained from SAXS results of the same specimens, are also listed in the table for comparison. The results of transmission electron microscopic (TEM) observation for the same specimens indicate that the morphology of the SB-4A is between lamellae and cylinder. For pure SB-4A the domain size determined by NMR is in agreement with that by SAXS.

The results of spin diffusion in PS/SB-4A blends indicate that the addition of PS into SB-4A has a distinct effect on the interdomain sizes of the SB-4A; hence, the domain sizes determined by NMR are markedly different from those by SAXS. As discussed above, low molecular weight PS03 not only solubilizes into the PS block domain but also solubilizes into the PBD domain. The sizes of pure PBD domains are decreased by the PS03 added. It is reasonable to consider that the amount of PS dissolved in PBD domains may be too little to be detected by SAXS but enough to accelerate the spin diffusion rate. However, most PS added are mixed with the PS block phase; hence, the interdomain sizes, determined by SAXS, are larger than those of pure SB-4A. NMR is very sensitive to the change of local environments; therefore, it can reveal the effect of the added PS on the PBD domains. For PS100/SB-4A blends, the situation is quite different from that of PS03/SB-4A blends. The PS100 added forms its own domain in between the PS block domains. The homogeneous PS100 domains cannot scatter the X-rays; hence, there is no effect on the SAXS results. As a result, the domain size of the blends determined by SAXS is the same as that of pure SB-4A. However, the magnetization of the PBD domain diffuses not only into the PS block domain but also into the PS domains; hence, the spin diffusion rate becomes smaller, and the interdomain size of the blend, determined by NMR, is larger than that of pure SB-4A. Therefore, NMR is a more sensitive technique for detecting microstructures of polymer systems than SAXS. The results obtained by NMR are more precise than those obtained by SAXS.

**Table 5. Domain Properties of SBS and Its Blends<sup>a</sup> with PS**

material	domain properties			
	$D^b$ (nm)	$t^b$ (nm)	$D^c$ (nm)	$t^c$ (nm)
SBS	27.1	$2.4 \pm 0.2$	30.8	$2.4 \pm 0.2$
PS03/SBS	17.1	$1.6 \pm 0.2$	32.2	$2.3 \pm 0.3$
PS1/SBS			34.6	$2.5 \pm 0.2$
PS100/SB-4A	31.2	$2.2 \pm 0.2$	30.09	$2.5 \pm 0.2$

<sup>a</sup> Composition of PS/SBS: 20:80. <sup>b</sup> Determined by proton spin diffusion. <sup>c</sup> Determined from SAXS.

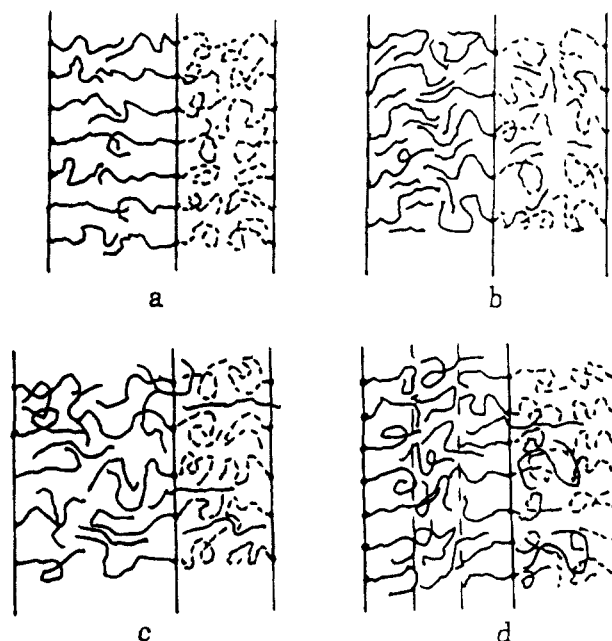


**Figure 5.** Schematic representations of the spatial segmental distribution of the block copolymer SB-4A and homopolymer chains in a microdomain space for different states of solubilization: (a) pure SB-4A block copolymer; (b) uniform solubilization of PS of very low  $M_{\text{PS}}$  in the PS block and PBD domains; (c) solubilization of PS with  $M_{\text{PS}}$  equal to or slightly larger than  $M_{\text{BPS}}$  in PS block domains; (d) localized solubilization of PS with  $M_{\text{PS}}$  much higher than  $M_{\text{BPS}}$  in the center of the PS block domains.

**C. Microstructures of the SBS and Its Blends with PS.** SAXS and proton spin diffusion were used to detect the interdomain sizes of SBS and its blends with PS. The results were listed in Table 5, which are similar to those of the PS/SB-4A blends. These results once again indicate that when the PS blocks locate at the outer ends of the SB block copolymer chains, the molecular architectures of the SB block copolymers have little effect on the morphological structures of the SB block copolymer/PS blends, as compared to the molecular weights of PS.

## Conclusion

Both SAXS and NMR results for SB-4A and SBS and their blends with PS can lead to the following conclusions: (1) SB-4A and SBS and their blends with PS of different  $M_{\text{PS}}$  have very regularly ordered domain structures. Quantitative analysis of the SAXS results indicates that the interdomain distance of the miscible blends increases with an increase in  $M_{\text{PS}}$  and that of the partially miscible blends is independent of  $M_{\text{PS}}$ . Moreover, the interfacial thickness of these blends is almost not dependent on the  $M_{\text{PS}}$ . (2) The results from proton spin diffusion measurements for pure block copolymers are in good agreement with those from SAXS. However, the NMR results about the blends

indicate that the interdomain size of PS03/SB-4A is decreased by the addition of PS03, suggesting that there is detectable quantity of PS03 dissolving in PBD microdomains, which hence decreases the size of pure PBD interdomains. On the contrary, the interdomain size of PS100/SB-4A is enlarged by the addition of PS100, as most of the added PS100 do not solubilize in the PS block domains but locate among the PS block domains. The above conclusions are rather different from those of SAXS but are in excellent agreement with those from DMA.<sup>1</sup> (3) The morphological structures of SBS and its blends with PS are similar to those of SB-4A and its blends with PS, indicating that the molecular architectures of the studied SB block copolymers have little effect on the morphological structures of their blends.

From the results mentioned above the possible morphological structures of the PS/SB-4A and PS/SBS blends are depicted in Figure 5.

**Acknowledgment.** The authors are grateful for the financial support granted by the National Basic Research Project—Macromolecular Condensed State, the National Natural Science Foundation of China, and the Laboratory of Magnetic Resonance and Atomic and Molecular Physics, Wuhan Institute of Physics, Chinese Academy of Sciences.

## References and Notes

- (1) Part 1: Feng, H.; Feng, Z.; Yuan, H.; Shen, L. *Macromolecules*, previous paper in this issue.
- (2) Hashimoto, T.; Shibayama, M.; Kawai, H. *Macromolecules* **1980**, *13*, 1237.
- (3) Hashimoto, T.; Fujimura, M.; Kawai, H. *Macromolecules* **1980**, *13*, 1660.
- (4) Shibayama, M.; Hashimoto, T. *Macromolecules* **1986**, *19*, 740.
- (5) Hashimoto, T.; Tanaka, H.; Hasegawa, H. *Macromolecules* **1990**, *23*, 4378.
- (6) Koizumi, S.; Hasegawa, H.; Hashimoto, T. *Macromolecules* **1990**, *23*, 2955.
- (7) Winey, K. I.; Thomas, E. L.; Fetters, L. J. *J. Chem. Phys.* **1991**, *95*, 9367.
- (8) Ruland, W. *J. Appl. Crystallogr.* **1971**, *4*, 70.
- (9) Porod, G. *Kolloid Z. Polym.* **1951**, *124*, 83; **1952**, *125*, 51 and 108.
- (10) Fava, R. A., Ed. *Methods of Experimental Physics*; Academic Press, Inc.: Troy, MO, 1980.
- (11) Hashimoto, T.; Nagatoshi, K.; Todo, A.; Hasegawa, H.; Kawai, H. *Macromolecules* **1977**, *10*, 2113.
- (12) Warner, F. P.; Macknight, W. J.; Stein, R. S. *J. Polym. Sci., Polym. Phys. Ed.* **1974**, *7*, 364.
- (13) Tanaka, H.; Nishi, T. *Phys. Rev.* **1986**, *B33*, 32.
- (14) Assink, R. A. *Macromolecules* **1978**, *11*, 1233.
- (15) Tekely, P.; Canet, D.; Puech, J. *J. Mol. Phys.* **1989**, *67*, 81.
- (16) Feng, H.; Feng, Z.; Ruan, H.; Shen, L. *Macromolecules* **1992**, *25*, 5981.
- (17) Havens, J. R.; VanderHart, D. L. *Macromolecules* **1985**, *18*, 1663.
- (18) Bondi, A. *J. Phys. Chem.* **1964**, *68*, 441.